JOURNAL OF SOLID STATE CHEMISTRY 68, 307–313 (1987)

Crystal Structure, Thermal Behavior, and Infrared Absorption Spectrum of Cesium Hydrogen Selenite–Selenious Acid (1/2) $CsHSeO_3 \cdot 2H_2SeO_3$

LASSI HILTUNEN AND JORMA HÖLSÄ*

Department of Chemistry, Helsinki University of Technology, SF-02150 Espoo, Finland

AND ZDENEK MIČKA

Department of Inorganic Chemistry, Charles University, 12840 Prague 2, Czechoslovakia

Received June 24, 1986

The present work describes the crystal structure, thermal behavior, and infrared absorption spectrum of cesium hydrogen selenite–selenious acid (1/2), $CsHSeO_3 \cdot 2H_2SeO_3$. This compound crystallizes in the monoclinic crystal system with $P2_1/c$–C_{2h}^5 ($Z = 4$) as the space group. The unit cell dimensions are as follows: $a = 8.9897(20)$, $b = 8.5078(21)$, $c = 12.6476(31)$ Å, and $\beta = 95.141(19)°$. The crystal structure consists of discrete H_2SeO_3 molecules which are weakly hydrogen bonded to form layers which are further connected by $(HSeO_3)^-$ ions with much stronger hydrogen bonds. The hydrogen atoms show no disorder within the hydrogen bonds. The Cs^+ ions are coordinated to oxygens from both selenious acid molecules and hydrogen selenite ions. The thermal decomposition of $CsHSeO_3 \cdot 2H_2SeO_3$ in air starts with incongruent melting due to rupture of hydrogen bonds at 310 K and is followed later by the formation of cesium diselenite phase. At higher temperatures (700 K) this compound decomposes with oxidation of selenium to yield cesium selenate. Both deformation and stretching vibrations of SeOH groups from both $(HSeO_3)^-$ ions and H_2SeO_3 molecules can be found in the IR absorption spectrum of $CsHSeO_3 \cdot 2H_2SeO_3$. This confirms the ordered position of hydrogen atoms in hydrogen bonds. The OH vibrations corresponding to hydrogen bonded species can be found also.

Introduction

The alkali metal hydrogen selenite–selenious acid (1/1) compounds, $MHSeO_3 \cdot H_2SeO_3$, constitute a group of materials with interesting physical and electrical properties. In the study of these compounds most attention has been directed to the clarification of the behavior of the hydrogen atoms in the hydrogen bonds from the point of view of their ordering, since they exert a decisive effect on the dielectric properties. In the paraelectric phase of these compounds the hydrogen atoms have often been found to be disordered in half-occupied positions in the hydrogen bonds. A typical case of such a compound is $CsHSeO_3 \cdot H_2SeO_3$ described by Tellgren and Liminga (*1*). A series of studies have been initiated in order to find out whether

* To whom all correspondence should be addressed.

0022-4596/87 $3.00

other alkali metal selenites possess properties similar to $MHSeO_3 \cdot H_2SeO_3$, e.g., ferro- or antiferroelectricity.

This study employs the results of the study of the solubility diagram of the Cs_2SeO_3–H_2SeO_3–H_2O system. In this study (*2*) three hydrogen selenites, $CsHSeO_3$, $CsHSeO_3 \cdot H_2SeO_3$, and $CsHSeO_3 \cdot 2H_2SeO_3$, were found. The first two compounds have already been described (*3*) in the literature and their molecular spectra (*4–6*) as well as their thermoanalytical properties have been evaluated (*7*). The crystal structure of $CsHSeO_3 \cdot H_2SeO_3$ has been determined, also (*8, 9*). As far as $CsHSeO_3 \cdot 2H_2SeO_3$ is concerned, the behavior of hydrogens in the hydrogen bonds has not yet been resolved. The main emphasis of this work is on the study of the IR spectra, the thermoanalytical properties, and the crystal structure of $CsHSeO_3 \cdot 2H_2SeO_3$. The present study is a continuation of the systematic study of selenites conducted both in the Department of Inorganic Chemistry of Charles University in Prague and in the Department of Chemistry of the Helsinki University of Technology.

Experimental

The cesium hydrogen selenite–selenious acid (1/2) compound, $CsHSeO_3 \cdot 2H_2SeO_3$, was prepared with the aid of the solubility data on the Cs_2SeO_3–H_2SeO_3–H_2O system. The colorless crystals obtained from a mixture containing 2.1 g $Cs_2SeO_3 \cdot H_2O$, 6.5 g SeO_2, and 1.0 g H_2O were filtered and subsequently washed with chloroform and dried in air at ambient temperature. The deuterated salt, $CsDSeO_3 \cdot 2D_2SeO_3$, was prepared analogously using $Cs_2SeO_3 \cdot D_2O$, SeO_2, and D_2O as the reactants. The compounds obtained were analyzed gravimetrically: selenium by the Bode method (*10*) and cesium as Cs_2PtCl_6. The results were consistent with the given formula.

The X-ray diffraction data collection was carried out with a Syntex $P2_1$ four-circle single crystal diffractometer at ambient temperature. Two standard reflections were chosen in order to verify the crystal and electronic stability. The intensity of these reflections tended to increase as the exposure time to X-ray radiation increased. This phenomenon was taken as an indication of the gradual degradation of the crystal observed visually, too. 2799 unique reflections were collected with $\sin\theta/\lambda$ less than 0.7 $Å^{-1}$. The intensities were corrected for Lorentz and polarization effects. The empirical absorption correction carried out on the data resulted in increased R values and was thus proved unsuccessful. Consequently, no absorption correction was used. Additional information about the data collection can be found in Table I.

The thermal behavior of $CsHSeO_3 \cdot 2H_2SeO_3$ was studied using thermogravimetry (TG), differential thermal analysis

TABLE I

SUMMARY OF CRYSTAL DATA, INTENSITY COLLECTION, AND STRUCTURE REFINEMENT FOR $CsHSeO_3 \cdot 2H_2SeO_3$

A. Crystal data	
Formula	$CsHSeO_3 \cdot 2H_2SeO_3$
Molecular weight	518.82
Crystal system	Monoclinic
Space group	$P2_1/c$–C_{2h}^5
a (Å)	8.9897(20)
b (Å)	8.5078(21)
c (Å)	12.6467(31)
β (degrees)	95.141(19)
V (Å^3)	963.36
Z	4
d_{calc} (g cm^{-3})	3.577
Radiation	MoK_α (λ = 0.71069 Å)
μ(MoK_α) (cm^{-1})	146.87
B. Data collection and structure refinement	
Ω scan collection	speed: variable
No. of data collected	2799
No. of unique data ($F_{obs} > 6\sigma(F_{obs})$)	2200
Absorption correction	No correction (see text)
Structure solution	Patterson methods[a]
No. of variables	119
R (%)	5.0
R_w (%)	4.9

[a] Computations were carried out using MITHRIL (*11*) and SHELX (*12*) programs.

(DTA), and differential scanning calorimetry (DSC). A method which gradually increased temperatures was used as well. The simultaneous recording of the TG and DTA curves in a static air atmosphere was carried out with a MOM Derivatograph OD 102 instrument in the temperature range 298 to 870 K using a heating rate of 5° min^{-1}. Complementary TG curves were recorded with a Perkin–Elmer TGS-2 apparatus using smaller sample weights (ca. 5 mg) and a dynamic air atmosphere with heating rates of 2.5 and 10° min^{-1}. The DSC measurements were carried out with a Perkin–Elmer DSC-4 scanning calorimeter through the temperature range 298 to 670 K with a heating rate of 10° min^{-1}. Additional thermoanalytical data were obtained using the gradually increased temperature method. The samples were then heated in a regulated electric oven increasing the temperature by 10° in 24 hr from 298 to 720 K. The intermediate products were constantly analyzed by IR spectroscopical and X-ray diffractometric methods.

The infrared spectra were obtained with an UR 20 apparatus between 400 and 4000 cm^{-1} using the Nujol mull technique. The measurements in the region from 1600 to 4000 cm^{-1} were also carried out using the tripene suspension method.

Crystal Structure of $CsHSeO_3 \cdot 2H_2SeO_3$

The position of the cesium atom was determined from the Patterson map and the positions of the selenium and oxygen atoms were subsequently found from the difference Fourier calculations with the aid of X-ray diffraction structure determination program MITHRIL (*11*). No hydrogen atoms were found. The full-matrix least-squares refinement of the atomic positions was carried out using the SHELX program (*12*). This refinement was based on 2200 reflections with F_{obs} greater than $6\sigma(F_{obs})$ and the reflections were weighted inversely proportional to the estimated variance. All atoms found were refined with anisotropic temperature factors to yield the final agreement factors R and R_w equal to 5.0 and 4.9%, respectively. The relatively high R values reflect the gradual degradation of the sample during the measurements. The accuracy of the final information about the crystal structure was, however, not substantially influenced. Details of the crystal data and the structure refinement are given in Table I.

The final positional parameters as well as the equivalent temperature factors are presented in Table II. The listings of the observed and calculated structure factors as well as the anisotropic thermal parameters are available from the authors upon request.

The crystal structure of $CsHSeO_3 \cdot 2H_2SeO_3$ is illustrated in Figs. 1 to 3. The bond angles and distances are listed in Table III. The projection of the crystal structure on the xz plane is shown in Fig. 1. The

TABLE II

FRACTIONAL POSITIONAL PARAMETERS AND EQUIVALENT TEMPERATURE FACTORS FOR $CsHSeO_3 \cdot 2H_2SeO_3$

Atom	x	y	z	U_{eq}[a] (Å^2)
Cs	0.7424(1)	0.2573(1)	0.9952(1)	3.41(3)
Se1	0.2657(1)	0.2646(1)	0.5354(1)	2.42(4)
Se2	0.5143(1)	0.4388(1)	0.2341(1)	2.62(4)
Se3	0.0294(1)	0.0443(1)	0.2641(1)	3.02(4)
O1	0.4015(6)	0.1455(7)	0.5063(5)	3.5(3)
O2	0.2473(6)	0.3911(6)	0.4346(5)	3.1(3)
O3	0.1073(7)	0.1454(7)	0.4957(5)	3.9(4)
O4	0.5229(7)	0.6299(7)	0.1825(5)	3.4(3)
O5	0.6890(7)	0.3873(8)	0.2384(6)	4.6(4)
O6	0.4963(7)	0.4985(7)	0.3642(5)	3.7(3)
O7	0.0097(6)	−0.1264(7)	0.3207(5)	3.1(3)
O8	−0.1539(8)	0.1107(7)	0.2773(5)	4.5(4)
O9	0.0111(7)	−0.0015(7)	0.1304(5)	3.7(4)

[a] The equivalent temperature factor U_{eq} was calculated from the anisotropic temperature factors with the aid of the following formula: $U_{eq} = \frac{1}{3}\Sigma_i\Sigma_j U_{ij} a_i^* a_j^* \mathbf{a}_i \cdot \mathbf{a}_j$. The U_{eq} values presented above were multiplied by a factor of 100.

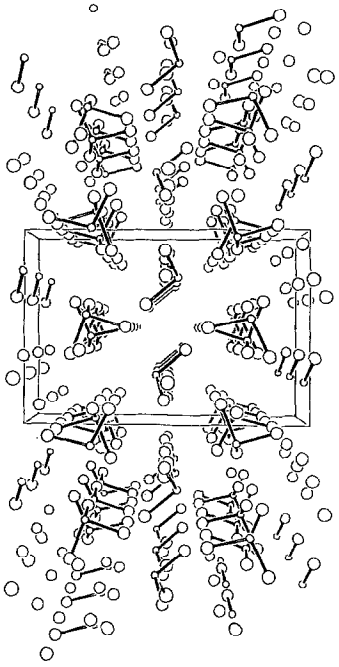

FIG. 1. Perspective view of the crystal structure on the xz plane.

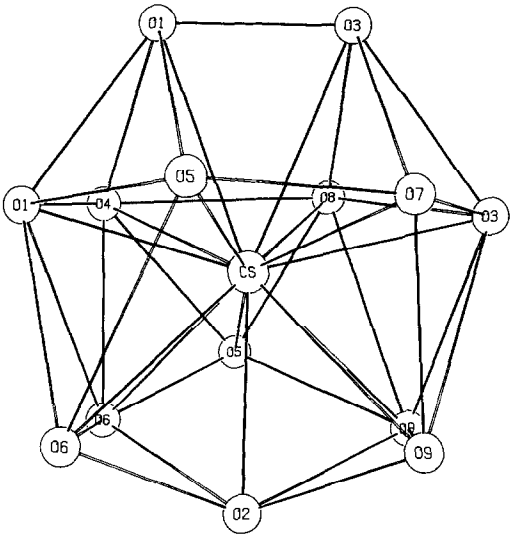

FIG. 3. The immediate environment of the Cs^+ ion in $CsHSeO_3 \cdot 2H_2SeO_3$.

Cs^+ and $(HSeO_3)^-$ ions on one hand and the H_2SeO_3 molecules on the other form layers perpendicular to the z axis. This long-range ordering in the structure is shown in Fig. 2. The adjacent H_2SeO_3 layers are linked by strong hydrogen bonds through the

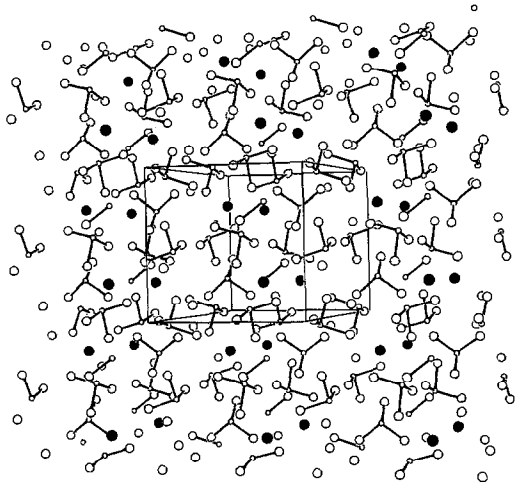

FIG. 2. Perspective view of the crystal structure of $CsHSeO_3 \cdot 2H_2SeO_3$ showing the layered structure. Filled circles represent the cesium atoms, small open ones the selenium atoms, and the large open ones oxygens.

TABLE III

BOND DISTANCES (IN Å) AND ANGLES (IN DEGREES) IN $CsHSeO_3 \cdot 2H_2SeO_3$

Cs–O1	3.190(6)	Cs–O6	3.422(6)
Cs–O8	3.190(7)	Cs–O5	3.465(8)
Cs–O7	3.233(6)	Cs–O1	3.547(6)
Cs–O2	3.238(5)	Cs–O3	3.566(6)
Cs–O4	3.271(6)	Cs–O9	3.578(6)
Cs–O5	3.344(8)	Cs–O9	3.586(6)
Cs–O3	3.383(6)	Cs–O6	3.646(6)
Se1–O1	1.653(6)	O1–Se1–O2	104.5(3)
Se1–O2	1.666(6)	O1–Se1–O3	100.1(3)
Se1–O3	1.783(6)	O2–Se1–O3	97.5(3)
Se2–O4	1.755(6)	O4–Se2–O5	100.8(3)
Se2–O5	1.627(6)	O4–Se2–O6	95.3(3)
Se2–O6	1.744(6)	O5–Se2–O6	102.6(3)
Se3–O7	1.636(6)	O7–Se3–O8	96.0(3)
Se3–O8	1.764(7)	O7–Se3–O9	103.0(3)
Se3–O9	1.728(6)	O8–Se3–O9	99.0(3)
O1 · · · O4	2.543(9)	O3 · · · O7	2.636(9)
O2 · · · O6	2.644(8)		
O2 · · · O9	2.562(8)	O5 · · · O8	2.766(9)

$(HSeO_3)^-$ groups. In contrast to the preceding, the H_2SeO_3 molecules within the layers are connected with weaker hydrogen bonds, as the O · · · O distances in Table III suggest.

The immediate surroundings of the cesium ions contain as many as 14 oxygens both from $(HSeO_3)^-$ ions and from H_2SeO_3 molecules (Fig. 3). The oxygens around cesium do not form any regular coordination polyhedra. The shortest Cs–O distance is 3.190 Å and the longest one is 3.646 Å, with an average of 3.404 Å (cf. Table III). Although all oxygens lie well within the distance of the sum of the van der Waals radii of the cesium and oxygen ions, it seems quite exaggerated to suggest that all the oxygens are coordinated to the cesium ion. In any case, there must be interactions between cesium and oxygens to some extent, although the strength of the contact may vary considerably.

The SeO_3 coordination polyhedra approach to the distorted trigonal pyramids with average O–Se–O angles around 100° for all three SeO_3 species present in the structure. One SeO_3 group shows two short Sc–O distances (1.656 and 1.666 Å) whereas the two other groups have only one short distance each (1.627 and 1.636 Å). In all cases the difference between the two groups of Se–O distances is clear, close to 0.1 Å, indicating the presence of discrete Se–O and Se–OH bonds and consequently the presence of one ionic $(HSeO_3)^-$ and two molecular H_2SeO_3 species. The situation differs from that in $CsHSeO_3 \cdot H_2SeO_3$ (*9*), where all Se–O distances were found to have intermediate values between the typical Se–O and Se–OH distances (ca. 1.65 and 1.75 Å, respectively). This phenomenon was interpreted as an indication of disorder in the position of the hydrogen atoms between the hydrogen bonded oxygens. According to the present study similar disorder evidently does not occur in $CsHSeO_3 \cdot 2H_2SeO_3$.

The hydrogen bonding has, however, some effect on the Se–O distances which involve hydrogen bonded oxygens—either simple oxygen or one from a hydroxy group. The most prominent examples are the stretched Se–O distances in the $(HSeO_3)^-$ group where all oxygens are relatively strongly hydrogen bonded. The lengthening of the Se1–O bonds increases the average Se1–O distance (1.701 Å) to nearly the mean values for the H_2SeO_3 molecules (both 1.709 Å). In the $(HSeO_3)^-$ group the only Se–O distances with oxygens not involved in hydrogen bonding, Se2–O5 and Se3–O9, are very short indeed when compared to the typical values of Se–O and Se–OH distances.

Several hydrogen bonds exist in the structure. As mentioned above four of them involve the oxygens of the hydrogen selenite ion and are relatively strong (O · · · O distances between 2.543 and 2.644 Å). These bonds are responsible for the linking of the H_2SeO_3 molecule layers. Weaker hydrogen bonds (O · · · O distances greater than 2.77 Å) connect the individual H_2SeO_3 molecules within the layer.

Thermal Behavior of $CsHSeO_3 \cdot 2H_2SeO_3$

Thermal decomposition of $CsHSeO_3 \cdot 2H_2SeO_3$ in air starts at 310 K with incongruent melting of the compound (cf. Table

TABLE IV

RESULTS OF TG, DTA, AND DSC MEASUREMENTS ON $CsHSeO_3 \cdot 2H_2SeO_3$

TG weight loss (%) *T*/K	DTA effect *T*/K	DSC effect *T*/K	Assignment
	endo 310–330	endo 320–330	Incongruent melting
8.50 330–430	endo 400–430	endo 340–390	Decomposition to diselenite and evaporation of H_2O and SeO_2
60.15 510–820	endo 540–570 650–700	endo 420–570	Sublimation of SeO_2 and decomposition and oxidation to selanate

IV). This is due to the destruction of hydrogen bonds connecting the selenite groups. Further decomposition takes place in the temperature range between 330 and 430 K with the liberation of selenium dioxide and water. Subsequently, cesium diselenite, $Cs_2Se_2O_5$, is formed. When the temperature is further increased sublimation of selenium dioxide occurs followed by decomposition of $Cs_2Se_2O_5$ which is accompanied by the oxidation of selenium yielding cesium selenate Cs_2SeO_4 at the temperature of 700 K.

The decomposition scheme can be presented as follows:

$$2CsHSeO_3 \cdot 2H_2SeO_3 \xrightarrow{-5H_2O,\ -4SeO_2}$$

$$Cs_2Se_2O_5 \xrightarrow{-SeO_2,\ \text{oxidation}} Cs_2SeO_4$$

A change of the heating rate does not influence substantially the decomposition scheme; the decomposition temperatures only shift higher with increasing heating rate. The shift in the temperature range corresponding to the sublimation of selenium dioxide is most pronounced.

The gradually increased temperature method was employed in order to elucidate the decomposition mechanism. The intermediate products were characterized with the aid of classical analytical methods, X-ray powder diffraction, and infrared spectroscopy. The results obtained by this method confirmed the fact that the other cesium hydrogen selenites, i.e., $CsHSeO_3$ and $CsHSeO_3 \cdot H_2SeO_3$, cannot be obtained as intermediate decomposition products of $CsHSeO_3 \cdot 2H_2SeO_3$ due to their low decomposition temperature (*7*).

Infrared Spectrum of $CsHSeO_3 \cdot 2H_2SeO_3$

The absorption frequencies observed in the IR spectrum of $CsHSeO_3 \cdot 2H_2SeO_3$ are reproduced in Table V. The assignment of the bands was based on data presented in the literature (*4, 13–15*).

TABLE V

IR Absorption Frequencies for $CsHSeO_3 \cdot 2H_2SeO_3$ (Compound I) and $CsDSeO_3 \cdot 2D_2SeO_3$ (Compound II) in the Range of 400 to 4000 cm^{-1}

$\tilde{\nu}_I$ (cm^{-1})	$\tilde{\nu}_{II}$ (cm^{-1})	$\tilde{\nu}_I/\tilde{\nu}_{II}$	Assignment
2600–3400 s, b (max 2750 and 3270)	1950–2500 s,b (max 2100 and 2450)	1.33 1.00	
2000–2500 s,b (max 2450)	1700–1900 s, b (max 1800)	1.35	ν(OX)
1650 w,b	1250 w,b	1.32	
1248 m	925 sh	1.34	
1170 w 1050 m			δ(OX)
886 sh	895 m	0.99	$\nu_3(A')XSeO_3^-$
860 s	860 s	1.00	
824 m	833 m	0.99	$\nu_1(A')X_2SeO_3$
770 sh	775 s	0.99	$\nu_3(A'')XSeO_3^-$
725 s	725 m	1.00	$\nu_3(A')X_2SeO_3$
678 s	683 s	0.99	$\nu_3(A'')X_2SeO_3$
653 s	660 s	0.99	
615 s	615 s	1.00	$\nu_1(A'')XSeO_3^-$
432 s	427 s	1.01	$\nu_2(A'')XSeO_3^-$ $\nu_2(A'')X_2SeO_3^-$

Note. intensity scale: w, weak; m, medium; s, strong, b, broad; sh, shoulder. X = H or D.

The deformation vibrations of the selenite anions are located in the region between 400 and 450 cm^{-1} and the stretching frequencies are situated in the region between 600 and 900 cm^{-1}. In the region of the stretching vibrations of the selenite anions absorption bands were found, indicating the presence of the $(HSeO_3)^-$ (615 and 860 cm^{-1}) and H_2SeO_3 (678, 725, and 824 cm^{-1}) groups in the structure. This observation confirms the results of the X-ray diffraction structure analysis presented above. The hydrogen atoms are located asymmetrically along the SeO–H · · · O hydrogen bonds in ordered positions at the lowest discrete levels of the two-minima asymmetrical potential function with a practically zero probability of tunneling (*16*). Consequently, the

broad absorption band with a maximum at 800 cm^{-1} corresponding to the presence of the selenite anion with hydrogen atoms in nonordered positions (*15*) is completely absent in the spectrum.

In the IR spectrum peaks corresponding to the OH vibrations are found also. These peaks originate from the hydrogen selenite ions involved in hydrogen bonding. The three absorption bands (at 1050, 1170 and 1248 cm^{-1}) are found in the region of the deformation vibrations of the SeOH group and can be thus assigned to hydrogen bonds of different strength with the hydrogen atoms in ordered positions (*17*). In the region of the stretching vibrations of the SeOH group the number (3), position, and shape of the bands are all very similar to other hydrogen selenites of the alkali metals. The spectrum is also similar to the spectra of the other acidic salts belonging to the ferroelectrics of potassium dihydrogen phosphate type (*16*). The similarity of the spectra of these compounds, differing in the number and the strength of the hydrogen bonds, is due to the slow interhydrogen bond tunneling effect (*15*, *16*, *18*).

Acknowledgment

Financial aid to one of the authors (J.H.) from the Academy of Finland is gratefully acknowledged.

References

1. R. Tellgren and R. Liminga, *Ferroelectrics* **8,** 629 (1974).
2. Z. Mičcka and M. Ebert, *Chem. Zvesti,* in press.
3. J. W. Mellor, *in* "A Comprehensive Treatise on Inorganic and Theoretical Chemistry (J. W. Mellor and G. D. Parkes, Eds.), Vol. X, Longmans, Green, NY London (1930).
4. C. A. Cody and R. C. Lewit, *J. Solid State Chem.* **26,** 281 (1978).
5. L. M. Rabkin, V. P. Dimitrijev, and L. A. Shuvalov, *Ferroelectrics* **14,** 627 (1976).
6. C. A. Cody and R. K. Khanna, *in* Proceedings, Int. Conf. Light Scatt. Solids," p. 932 (1975).
7. Z. Mička, thesis, Charles University, Prague (1982).
8. S. Sato, *J. Phys. Soc. Japan* **32,** 1670 (1972).
9. S. Chomnilpan, R. Tellgren, and R. Liminga, *Acta Crystallogr. B* **34,** 373 (1978).
10. H. Bode, *Z. Anal. Chem.* **153,** 335 (1956).
11. C. J. Gilmore, "A Computer Program for the Automatic Solution of Crystal Structures from X-ray Data," University of Glasgow, Glasgow (1983).
12. G. M. Sheldrick, "Program for Crystal Structure Determination, University of Cambridge, Cambridge (1976).
13. A. Simon and R. Paetzold, *Z. Elektrochem.* **64,** 209 (1960).
14. A. Simon and R. Paetzold, *Z. Anorg. Allg. Chem.* **302,** 39 (1960).
15. C. A. Cody and R. C. Lewit, *J. Solid State Chem.* **26,** 293 (1978).
16. C. A. Cody and R. K. Khanna, *Indian J. Pure Appl. Phys.* **16,** 296 (1978).
17. P. K. Acharya and P. S. Narayana, *Spectrochim. Acta Part A* **29,** 925 (1973).
18. V. H. Schmidt and E. A. Uehling, *Phys. Rev.* **126,** 447 (1972).